

This is the accepted version of the document published at:

Blanco-Cano, L., Soria-Verdugo, A., Garcia-Gutierrez, L. M., & Ruiz-Rivas, U. (2016). Modeling the thin-layer drying process of granny smith apples: Application in an indirect solar dryer. *Applied Thermal Engineering*, 108, 1086-1094

DOI: <https://doi.org/10.1016/j.applthermaleng.2016.08.001>

© Elsevier, 2016



This work is licensed under a [Creative Commons Attribution-NonCommercial-NoDerivatives 4.0 International License](https://creativecommons.org/licenses/by-nc-nd/4.0/).

1 **Modeling the thin-layer drying process of Granny Smith apples: Application in an indirect**  
2 **solar dryer.**

3 L. Blanco-Cano<sup>a</sup>, A. Soria-Verdugo<sup>b\*</sup>, L.M. Garcia-Gutierrez<sup>b</sup>, U. Ruiz-Rivas<sup>a,b</sup>

4 a: Appropriate Technology Group b: Energy Systems Engineering

5 \*: corresponding author: [asoria@ing.uc3m.es](mailto:asoria@ing.uc3m.es)

6 Department of Thermal and Fluids Engineering. University Carlos III of Madrid.

7 Avda. Universidad 30, 28911, Leganés (Spain). Tel. +34916248465

8 **Abstract**

9 The thin-layer drying kinetics of Granny Smith apples is determined by thermogravimetric  
10 analysis of the drying process at constant temperatures ranging from 20 °C to 50 °C, using  
11 intervals of 5 °C. The experimental drying curves obtained in the TGA were fitted to the Wang-  
12 Singh equation, which was found to describe precisely the drying process. A novel model,  
13 capable of predicting the evolution of the moisture ratio of Granny Smith apples during the  
14 drying process and under variable drying temperatures, was proposed. The model was  
15 validated with experimental TGA measurements of the drying of apples at variable  
16 temperatures, typical of solar drying, obtaining maximum deviations for the drying time of less  
17 than 1.5%. Once validated, the model proposed was also applied to the drying of Granny Smith  
18 apples in an indirect solar dryer. The comparison of the model prediction with the  
19 experimental measurements of the drying of apples at variable drying conditions conducted in  
20 a lab-scale solar dryer showed a proper agreement, with low deviations (less than 10%) due to  
21 the thermal inertia of the samples.

22 **Keywords**

23 Solar drying; Granny Smith apples; Drying kinetics; Thin-layer drying; TGA; Mathematical  
24 model.

25 **1. Introduction**

26 Solar drying is a commonly used method for preservation or processing of a wide variety of  
27 agricultural products [1-3]. Apples are selected in this work as test products since they are an  
28 important raw material produced all around the world. Dried apples can be consumed directly  
29 or treated as a secondary raw material [4]. The variety of apples named Granny Smith is  
30 characterized by growing in areas with climates relatively warm [5] which makes this variety  
31 suitable for solar drying. Solar drying of different varieties of apples has been analyzed in the  
32 literature [6-8], but no experiences on Granny Smith have been found.

33 In indirect solar dryers, the drying process depends mainly on the drying conditions (air mass  
34 flow rate, and airflow temperature and relative humidity) in the drying chamber and on the  
35 drying kinetics of the product at those conditions. The drying conditions at the inlet of the  
36 drying chamber depend on the air heating process in the solar collector [9], and thus the  
37 drying process is highly dependent on the ambient conditions and the solar irradiance. While  
38 the solar drying process is characterized by variable drying conditions, the drying kinetics is  
39 generally studied at constant drying conditions.

40 The thin-layer drying is the procedure of drying one single layer of particles or slices of a  
41 product. The thin-layer equations predict the temporal evolution of the moisture content of  
42 the samples, based on empirical models of the drying process: Lewis, Page, Henderson and  
43 Pabis, Logarithmic, two terms, two terms exponential, Wang and Singh, among others [10].  
44 These models have been widely used in the study of the drying kinetics or to obtain the  
45 diffusion coefficient of several agricultural products [3, 11-15]. When the drying kinetics  
46 obtained at constant drying conditions are applied to the prediction of the evolution of a solar  
47 drying process, it is generally performed by means of mathematical simulation of the heat and  
48 mass transfer processes in the drying chamber [16, 17], which are simulations of high  
49 complexity. To the knowledge of the authors, there are no simple models available in the  
50 literature to predict the evolution of the moisture loss during the drying process at the variable  
51 drying conditions characteristic of solar drying processes.

52 Regarding the drying kinetics of apples, most of the works reported consist of the  
53 mathematical modeling of the drying curves obtained experimentally, employing the thin-layer  
54 equations at constant drying conditions, for different varieties of apples. The tests are typically  
55 conducted at different values of constant temperatures, and for different values of a second  
56 parameter, such as the sample thickness [18], the air velocity [19] the air relative humidity [20]  
57 or the temperature of the product [21]. Only a few researchers have focused on the drying  
58 kinetics of Granny Smith apples. Vega-Gálvez et al. [5] and Velic et al. [22] studied the drying  
59 kinetics in a range of temperatures between 40 °C and 80 °C. Doymaz [12] and González-Fésler  
60 et al. [23] reported the effect of different pre-treatments on the drying kinetics of Granny  
61 Smith apples at 60 °C and 65 °C respectively. However, these studies do not cover the whole  
62 range of temperatures of small-scale solar drying, which for Granny Smith application would  
63 be lower.

64 In this work, thin-layer drying tests were conducted in a TGA for several constant drying  
65 temperatures, obtaining the drying curves for Granny Smith apples. Different thin-layer  
66 equations available in the literature were fitted to the experimental drying curves obtained in  
67 the TGA. Then, a mathematical model capable of predicting the sample mass loss under  
68 variable temperatures is proposed and validated using TGA experimental results and  
69 experimental measurements obtained in a lab-scale solar dryer.

## 70 **2. Experimental Setup**

71 The experiments were conducted employing two different systems: a TGA and a lab-scale  
72 indirect solar dryer operated at controlled conditions. The lab-scale solar dryer can operate at  
73 either constant conditions or at the variable conditions corresponding to different climates. A  
74 characteristic climate of the harvest season of Granny Smith apples has been established and  
75 used as inlet conditions during the experiments. For the tests, fresh Granny Smith apples were  
76 employed.

### 77 **2.1. Determination of the ambient conditions**

78 In order to reproduce the solar drying process of Granny Smith apples during the drying  
79 experiments, the climate of the harvest season of a region in Spain where Granny Smith apples  
80 are cultivated is selected as the reference climate. The apples are typically harvested in that

81 region between the end of September and the beginning of October [24]. Data of solar  
 82 irradiance, temperature and relative humidity are available online [25]. In the indirect solar  
 83 dryer, air at ambient temperature and relative humidity is heated in the solar collector and  
 84 directed to the drying chamber. Hence, the characteristic parameters of the climate for  
 85 indirect solar drying applications are: the temperature and the relative humidity of ambient  
 86 air, and the solar irradiance.

87 The solar air collector is inclined an angle  $\beta$ . Hence, according to Duffie and Beckmann [26], the  
 88 solar irradiance on the collector angle is:

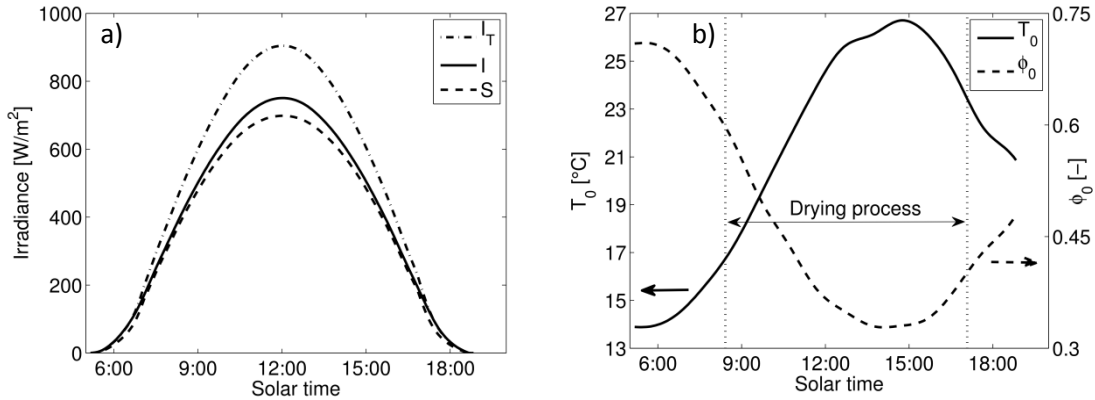
$$89 \quad I_T = I_b R_b + I_d \left( \frac{1 + \cos \beta}{2} \right) + I \rho_g \left( \frac{1 - \cos \beta}{2} \right) \quad (1)$$

90 where  $I_b$  and  $I_d$  are the beam and diffuse components of the solar irradiance,  $I$ , respectively.  $R_b$   
 91 is the ratio of beam irradiance on tilted surface to that on the horizontal plane, determined by  
 92 trigonometric relations, and  $\rho_g$  is the ground reflectivity. Hence, the irradiance on the tilted  
 93 surface,  $I_T$ , depends on the location of the air heater, the collector angle and the solar time.  
 94 Typical flat-plate solar collectors comprise an absorber plate and a glass cover [27]. Due to the  
 95 transmittance of the glass cover and the absorptance of the absorber plate, only a fraction of  
 96 the solar irradiation incident on the solar collector is absorbed by the absorber plate. The solar  
 97 irradiance absorbed by the absorber plate can be determined as [26]:

$$98 \quad S = I_b R_b (\tau\alpha)_b + I_d (\tau\alpha)_d \left( \frac{1 + \cos \beta}{2} \right) + I \rho_g (\tau\alpha)_g \left( \frac{1 - \cos \beta}{2} \right) \quad (2)$$

99 where  $(\tau\alpha)_b$ ,  $(\tau\alpha)_d$  and  $(\tau\alpha)_g$  are the effective transmittance-absorptance products, referred to  
 100 the beam, diffuse and reflected components, respectively, which depends on the materials of  
 101 the solar air heater.

102 The solar irradiance on the horizontal plane ( $I$ ) in a typical sunny day of the harvest season in  
 103 the location where the apples are harvested is presented in Figure 1 a) in solid line. The solar  
 104 irradiance on the collector angle ( $I_T$ ), shown in dashed-dotted line, is calculated for a collector  
 105 angle  $\beta = 20^\circ$ . The solar irradiance absorbed by the absorber plate ( $S$ ) that would be obtained  
 106 in a typical small-scale solar dryer is calculated for the typical materials used in solar drying  
 107 applications, and depicted in Figure 1 a) in dashed line. The solar irradiance absorbed by the  
 108 absorber plate can be determined approximately in this case as  $S \sim 0.95 \cdot I$ . The ambient air  
 109 temperature ( $T_0$ ) and relative humidity ( $\phi_0$ ) are shown in Figure 1 b). Since the solar dryer takes  
 110 the air from the ambient,  $T_0$  and  $\phi_0$  correspond to the air conditions at the inlet of the solar  
 111 dryer.



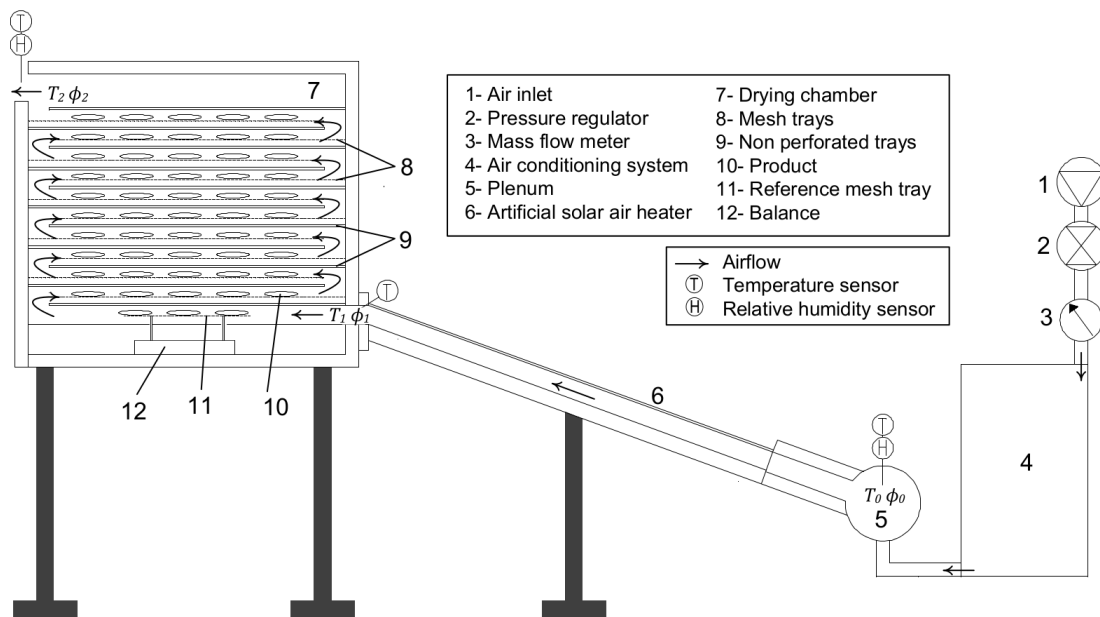
112  
113  
114  
115

Figure 1: Characteristic parameters of the reference climate: a) solar irradiance on the collector angle, on the horizontal surface and absorbed by the absorber plate and b) temperature and relative humidity of the ambient air.

116 The ambient conditions shown in Figure 1 represent the reference climate to be simulated in  
117 the lab-scale solar dryer to reproduce the solar drying process of the Granny Smith apples. The  
118 drying process is considered to start when the relative humidity of the ambient air lowers 60%  
119 (which in this case occurs approximately 2.5 hours after the sunrise) and ends when the solar  
120 altitude angle lowers 10°.

## 121 2.2. Lab-scale indirect solar dryer and measurement system

122 A lab-scale indirect solar dryer was employed to reproduce the drying conditions on field. The  
123 experimental facility is composed of an air conditioning system to establish a prescribed  
124 airflow temperature and relative humidity, an artificial indirect solar dryer that reproduces the  
125 solar drying process, and the measurement and control systems. A schematic of the lab-scale  
126 indirect solar dryer is shown in Figure 2.



127  
128

Figure 2: Schematic of the lab-scale indirect solar dryer.

129 The airflow is taken from the pneumatic air network (1) available in the laboratory. The air  
 130 conditioning system (4) establishes the required air temperature ( $T_0$ ) and relative humidity ( $\phi_0$ )  
 131 at the inlet of the solar collector. The airflow at temperature  $T_0$  and relative humidity  $\phi_0$  is  
 132 directed through the solar collector (6) to the drying chamber (7). An electrical resistance  
 133 heats the airflow in the solar collector, supplying a variable thermal power equal to the  
 134 product of the irradiance absorbed by the solar collector ( $S$ ) times the collector area ( $A_c$ ). The  
 135 air enters the drying chamber at temperature  $T_1$  and relative humidity  $\phi_1$ . The drying chamber  
 136 contains 13 non-perforated trays, arranged in series to maximize the airflow velocity around  
 137 the product. The thin-layer samples of Granny Smith apples are located on wired mesh trays  
 138 located between the non-perforated trays. The first tray lays on a balance that registers the  
 139 sample mass variation each 5 s. Hence, the first mesh tray is used as the reference tray.

140 The solar dryer dimensions are presented in Table 1. These dimensions are within the typical  
 141 range of small-scale indirect solar dryers. The walls and the bottom of the solar collector and  
 142 the drying chamber are thermally isolated.

143 Table 1: Solar dryer dimensions.

Solar dryer component	Dimension
Collector length [m]	1
Collector width [m]	0.5
Distance between the absorber plate and the glass cover [m]	0.045
Drying chamber length [m]	0.75
Drying chamber width [m]	0.5
Drying chamber height [m]	0.64
Distance between trays [m]	0.045

144

145 The apples used for the tests are washed, cut into slices of 2.4 mm and immersed in citric acid  
 146 to prevent oxidation [12]. The average total moisture content of the samples, determined for  
 147 25 samples dried in a Memmert UFE 500 oven, was 86.7%, with a standard deviation of 0.8%.

### 148 2.2.1. Measurement and control systems

149 The main characteristics of the measurement system are presented in Table 2, where the  
 150 details of the location of the sensors, the type and the accuracy of the sensor used are  
 151 reported. The air conditioning system and the power of the solar collector are controlled using  
 152 a PID controller.

153 Table 2. Measurement system characteristics of the indirect solar dryer.

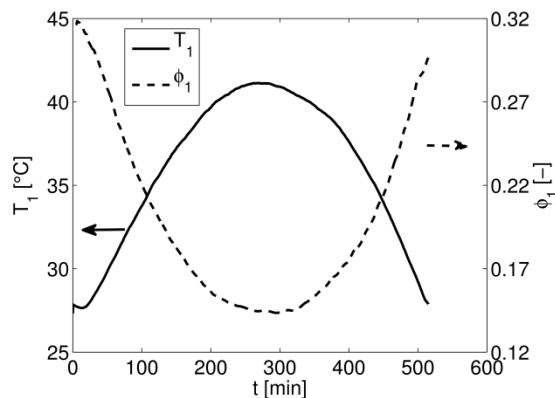
Measurement	Location	Type of sensor	Accuracy
Temperature of the airflow [°C]	Inlet of the collector	NTC thermistor	$\pm 0.3$
	Outlet of the collector	T-type	$\pm 1$

		thermocouple	
	Outlet of the drying chamber	NTC thermistor	$\pm 0.3$
Relative humidity of the airflow [%]	Inlet of the collector	Capacitive sensor	1.5
	Outlet of the drying chamber		
Air mass flow rate [kg/s]	Inlet of the air conditioning system	Air mass flow meter SMC®	$9 \cdot 10^{-4}$
Mass of the product during the drying process [g]	Drying chamber. Reference tray	Balance PCE® 3 kg	1
Power of the electric heater of the solar collector [W]	AC supply	Power transducer	$\pm 10$

154

### 155 2.2.2. Drying Conditions

156 For the climate considered (Figure 1), and operating with an air mass flow rate of 0.015 kg/s in  
 157 the lab-scale indirect solar dryer, the temperature and relative humidity of the airflow  
 158 obtained at the inlet of the drying chamber ( $T_1$  and  $\phi_1$ ) are presented in Figure 3. The drying  
 159 conditions shown in Figure 3 will be employed during the drying process of Granny Smith  
 160 apples at variable conditions in both the TGA and the indirect solar dryer tests.



161

162 Figure 3: Temperature and relative humidity obtained at the inlet of the drying chamber.

163 The rate of solar energy used is determined by the collector efficiency, calculated as the ratio  
 164 of useful heat absorbed by the airflow during the day to the total available solar irradiation.  
 165 The collector efficiency during the drying process, considering the temperature  $T_1$  depicted in  
 166 Figure 3, the ambient temperature  $T_0$  and the solar irradiance on the horizontal plane (Figure  
 167 1) is:

$$168 \quad \eta = \frac{\int \dot{m} c_p (T_1 - T_0) dt}{\int I A_c dt} = 0.65 \quad (3)$$

### 169 2.3. Thermogravimetric Analyzer

170 A thermogravimetric analyzer TGA Q500 from TA Instruments is used to obtain the drying  
171 kinetics of Granny Smith apples at isothermal conditions, and to reproduce the temperature  
172 profile ( $T_1$ ) shown in Figure 3. The inert gas employed was nitrogen, flowing through the  
173 furnace at a rate of 0.06 l/min. The TGA weighting precision is  $\pm 0.01\%$  and its sensitivity in the  
174 mass measurement is 0.1  $\mu\text{g}$ . The apple samples employed in the tests were cylinders of 1 cm  
175 in diameter and a thickness of 2.4 mm. The mass of the Granny Smith apples used in the TGA  
176 measurements is around 150 mg. Even though the apple samples do not become oxidized in a  
177 nitrogen stream, the samples were immersed in citric acid to present the same initial  
178 conditions as those of the tests in the solar dryer. For the determination of the drying kinetics,  
179 tests at temperatures ranging from 20 °C to 50 °C, using intervals of 5 °C, were conducted,  
180 covering the whole operating range shown in Figure 3.

181

### 182 **3. Mathematical model of the thin-layer drying process of Granny Smith apples**

183 In this section, the drying curve for Granny Smith apples was estimated using thin-layer drying  
184 equations for a range of temperature from 20 °C to 50 °C, a typical drying temperature range  
185 for solar dryers. Based on these results, a mathematical model capable of predicting the  
186 evolution of the drying process for variable air temperatures is proposed.

#### 187 **3.1. Thin-layer drying equations**

188 The drying process of biological products is governed by the diffusion mechanism of moisture  
189 during the falling rate period [28]. There are many equations available in the literature capable  
190 of predicting the evolution of the mass of the sample during the falling rate period of the  
191 drying process. The drying process is characterized by the moisture ratio,  $MR$ , a dimensionless  
192 parameter that quantifies the reduction of the moisture content of the sample with time [12,  
193 20, 28]. The moisture ratio is defined as:

$$194 \quad MR = \frac{M(t) - M_e}{M_0 - M_e} \quad (4)$$

195 where  $M(t)$  is the moisture content (wet basis) after a time  $t$ ,  $M_e$  is the equilibrium moisture  
196 content and  $M_0$  is the initial moisture content. The moisture ratio  $MR$  varies between  $MR = 1$ ,  
197 at the beginning of the drying process, and  $MR = 0$ , once the sample is dried at equilibrium  
198 with the drying air.

199 Different equations based on the thin-layer drying models available in the literature were used  
200 to model the evolution with time of the moisture ratio of Granny Smith apples dried at a  
201 constant temperature of 35 °C. The moisture loss was determined using the TGA and the  
202 moisture ratio was calculated using Eq. 4. The results were fitted to eleven different thin-layer  
203 drying equations. For the fitting procedure, the moisture ratio considered is between  $MR = 1$   
204 and  $MR = 0.1$ , since after that value, the drying rate decreases drastically and thus the samples  
205 are almost dry. Table 1 shows the equations proposed by different authors for the prediction  
206 of the moisture ratio during time, together with the values of the fitting parameters of each



207 equation obtained for the experimental results. The determination coefficient  $R^2$  of the  
 208 different fittings is also reported in the table.

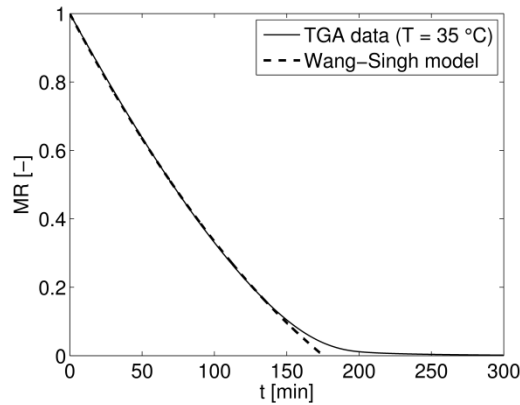
209 Table 1: Fitting parameters of different thin-layer drying equations available in the literature  
 210 applied to the moisture ratio obtained drying Granny Smith samples in TGA at 35 °C.  
 211 Valid for  $1 \geq MR \geq 0.1$ .

Equation	Model name	Parameters	$R^2$ [-]	Reference
$MR = 1 + a \cdot t + b \cdot t^2$	Wang and Singh	$a = -0.00794 \text{ min}^{-1}$ $b = 1.28 \cdot 10^{-5} \text{ min}^{-2}$	0.9999	[29]
$MR = \exp(-k \cdot t)$	Lewis	$k = 0.01074 \text{ min}^{-1}$	0.9865	[30]
$MR = \exp(-k \cdot t^n)$	Page	$k = 0.00257 \text{ min}^{-n}$ $n = 1.32$	0.9961	[31]
$MR = a \cdot \exp(-k \cdot t)$	Henderson and Pabis	$a = 1.078$ $k = 0.0118 \text{ min}^{-1}$	0.9798	[32]
$MR = a \cdot \exp(-k \cdot t) + c$	Logarithmic	$a = 1.888$ $k = 0.00441 \text{ min}^{-1}$ $c = -0.880$	0.9998	[18]
$MR = a \cdot \exp(-k_1 \cdot t) + b \cdot \exp(-k_2 \cdot t)$	Two terms	$a = 29.82$ $k_1 = 0.00255 \text{ min}^{-1}$ $b = -28.82$ $k_2 = 0.00236 \text{ min}^{-1}$	0.9999	[33]
$MR = a \cdot \exp(-k \cdot t) + (1-a) \cdot \exp(-k \cdot a \cdot t)$	Two terms exponential	$a = 1.846$ $k = 0.01629 \text{ min}^{-1}$	0.9952	[34]
$MR = a \cdot \exp(-k \cdot t) + (1-a) \cdot \exp(-k \cdot b \cdot t)$	Diffusion approximation	$a = -8.39$ $k = 0.01794 \text{ min}^{-1}$ $b = 0.9435$	0.9879	[35]
$MR = a \cdot \exp(-k_1 \cdot t) + (1-a) \cdot \exp(-k_2 \cdot t)$	Verma	$a = 4.823$ $k_1 = 0.00295 \text{ min}^{-1}$ $k_2 = 0.0016 \text{ min}^{-1}$	0.9998	[36]
$MR = a \cdot \exp(-k_1 \cdot t) + b \cdot \exp(-k_2 \cdot t) + c \cdot \exp(-k_3 \cdot t)$	Modified Henderson and Pabis	$a = -4.674$ $k_1 = 0.0339 \text{ min}^{-1}$ $b = 1.678$ $k_2 = 0.0509 \text{ min}^{-1}$ $c = 4.015$ $k_3 = 0.0215 \text{ min}^{-1}$	0.9989	[37]
$MR = a \cdot \exp(-k \cdot t^n) + b \cdot t$	Midilli	$a = 0.993$ $k = 0.00414 \text{ min}^{-n}$ $n = 1.13$ $b = -0.00135 \text{ min}^{-1}$	>0.9999	[38]

212 Based on the results shown in Table 1, and considering simplicity and accuracy criteria, the  
 213 equation selected for the prediction of the moisture ratio is that proposed by Wang and Singh  
 214 [29], which is a quadratic equation in the form:

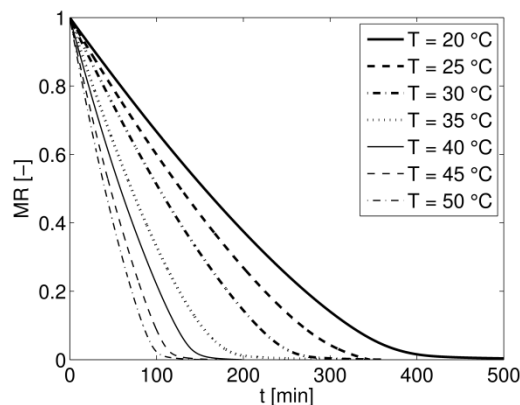
215  $MR = 1 + at + bt^2$  (5)

216 The moisture ratio as a function of time obtained in the TGA for the isothermal process at 35  
 217 °C is plotted in Figure 4 together with the fitting of Wang and Singh equation. The equation  
 218 proposed by Wang and Singh described precisely the drying process occurring in the TGA at  
 219 the temperature of 35 °C for moisture ratios above  $MR = 0.1$ , nevertheless the model is not  
 220 capable of predicting properly the drying process for moisture ratios below 0.1.



221  
 222 Figure 4: Moisture ratio obtained by the TGA at 35 °C and Wang and Singh equation fitting for  
 223 the moisture ratio above  $MR = 0.1$ .

224 Several drying processes of Granny Smith apples were conducted in the thermogravimetric  
 225 analyzer for constant temperatures ranging from 20 to 50 °C, using temperature intervals of 5  
 226 °C. Figure 5 shows the evolution of the moisture ratio ( $MR$ ) with time ( $t$ ) for the different  
 227 constant temperatures tested. The tendency of the moisture ratio is similar for all the  
 228 temperatures studied, but there is a strong effect of the temperature on the drying time ( $t_d$ ).



229  
 230 Figure 5: Evolution of the moisture ratio with time during the thin-layer drying of Granny Smith  
 231 apples in TGA.

232 **3.2. Mathematical model of the thin-layer drying process of Granny Smith apples at variable**  
 233 **temperature**

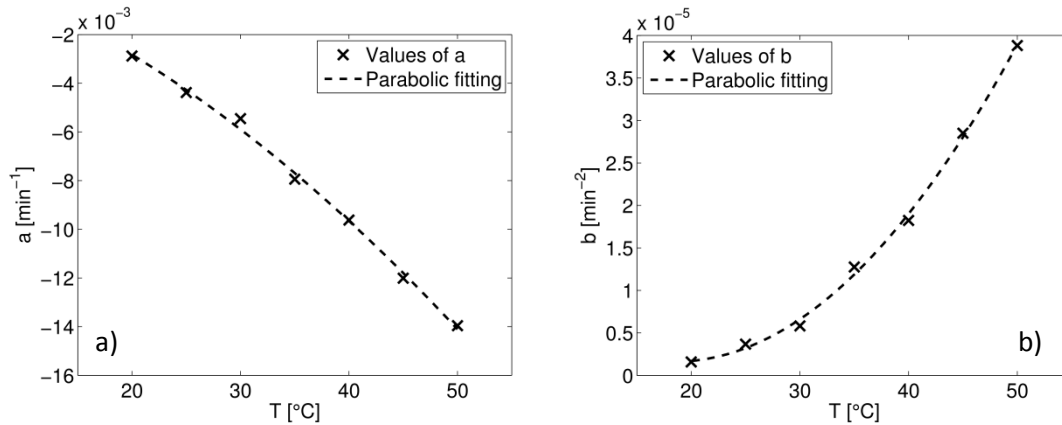
234 Following the procedure describe in Section 3.1, the equation proposed by Wang and Singh  
 235 [29] (Eq. 5) was employed to fit the evolution of the experimental moisture ratio with time  
 236 from  $MR = 1$  to  $MR = 0.1$ , for each temperature. The values of the free parameters  $a$  and  $b$  in  
 237 Eq. 2 obtained for each temperature are shown in Figure 6 a) and b) respectively, as a function  
 238 of the constant temperature employed during the drying process in the TGA. The values

239 obtained for  $a$  and  $b$  are plotted in Figure 6 together with a parabolic fitting, showing a proper  
 240 agreement of the fitting to the values. The determination coefficients of the fitting are  $R^2 =$   
 241  $0.997$  for  $a$  and  $R^2 = 0.998$  for  $b$ . The equations of the parabolic fitting for the parameters of  
 242 the equation proposed by Wang and Singh [29] for the temporal evolution of the moisture  
 243 ratio are:

$$244 \quad a = -3.44 \cdot 10^{-6} T^2 - 1.35 \cdot 10^{-4} T + 1.26 \cdot 10^{-3} \quad (6)$$

$$245 \quad b = 3.75 \cdot 10^{-8} T^2 - 1.39 \cdot 10^{-6} T + 1.44 \cdot 10^{-5} \quad (6)$$

246 where  $a$  is obtained in  $\text{min}^{-1}$  and  $b$  in  $\text{min}^{-2}$  for a temperature  $T$  in  $^{\circ}\text{C}$ .



247  
 248 Figure 6: Values of the free parameters of the equation proposed by Wang and Singh [29] for  
 249 the TGA measurements.

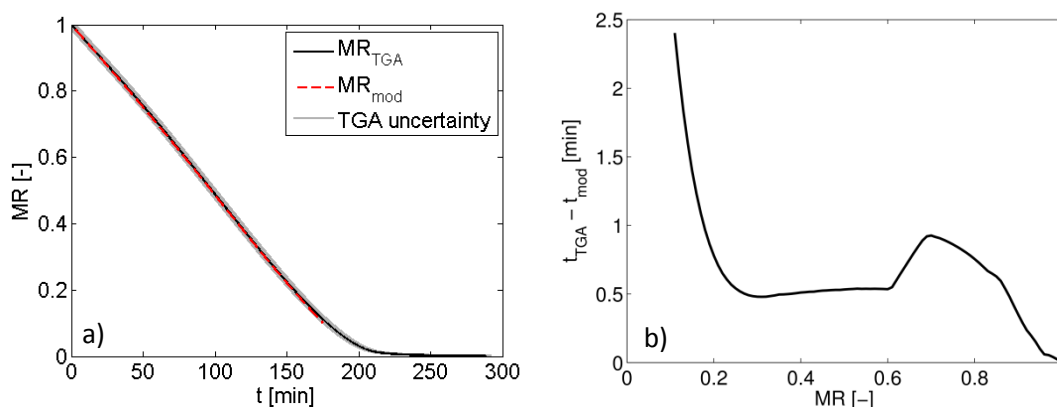
250 The values of  $a$  and  $b$  can be obtained for any temperature using respectively Eq. 6 and Eq. 7.  
 251 Hence a model is proposed to estimate the evolution of the moisture ratio during the thin-  
 252 layer drying process of Granny Smith apples conducted in a TGA under a variable temperature  
 253 profile. The model considers a quasi-steady drying process where the thermal inertia of the  
 254 sample is negligible. This assumption can be justified by the reduced size of the samples  
 255 employed in the TGA tests (mass sample under 150 mg). The time is discretized in small time  
 256 intervals ( $dt$ ) of 10 ms, and for each time ( $t = n \cdot dt$ ) the temperature is calculated. Using Eq. 6  
 257 and Eq. 7 the values of  $a$  and  $b$  are determined for the calculated temperature. Knowing the  
 258 value of  $MR$  estimated by the model at the beginning of the time interval, the values of  $a$  and  $b$   
 259 obtained are employed to determine the decrement of the moisture ratio ( $\Delta MR$ ) for the time  
 260 interval  $dt$ , considering the temperature constant during that short time period. Therefore, the  
 261 value of the moisture ratio at the end of the time interval  $dt$  is calculated as the value at the  
 262 beginning of the time interval minus the decrement of the moisture ratio, i.e.  $MR(t + dt) =$   
 263  $MR(t) - \Delta MR$ . The initial condition for the moisture ratio, at the beginning of the drying  
 264 process, is  $t = 0 \text{ s} \rightarrow MR = 1$ . The model estimates the evolution of the moisture ratio with time  
 265 for  $MR \geq 0.1$ .

## 266 4. Results and discussion

### 267 4.1. Validation of the thin-layer drying model

268 The model proposed for the thin-layer drying of Granny Smith apples at a variable temperature  
 269 was validated conducting a drying test in the TGA for variable drying temperatures. In order to  
 270 employ a realistic drying temperature, the temperature measured at the inlet of the drying  
 271 chamber in the lab-scale indirect solar dryer (Figure 3) was used to program the temperature  
 272 profile in the TGA. The temperature at the inlet of the drying chamber was obtained using the  
 273 operating conditions discussed in Section 2. Since the TGA Q 500 employed permits only to  
 274 program constant heating rates, i.e. linear temperature increases, the temperature measured  
 275 at the inlet of the drying chamber, shown in Figure 3, was divided into 30 linear temperature  
 276 increases, which were programmed in the TGA. Since the temperature in the TGA cannot be  
 277 controlled accurately during the cooling process, the test in the TGA ends once the maximum  
 278 temperature is reached, that is after around 300 min. Nevertheless, the apple sample is totally  
 279 dried ( $MR \rightarrow 0$ ) before 300 min.

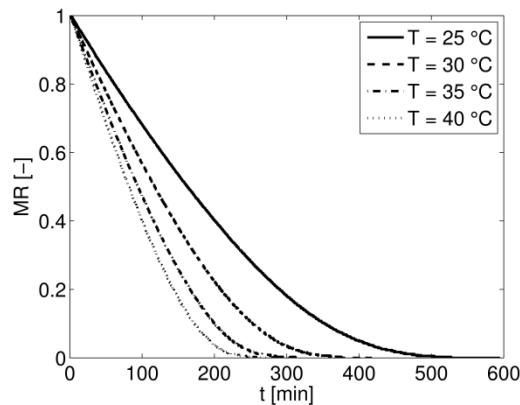
280 The model proposed in Section 3.2 was applied to the thin-layer drying process of the Granny  
 281 Smith apple samples in the TGA, subjected to the temperature profile showed in Figure 3. The  
 282 experimental value of the moisture ratio obtained in the TGA ( $MR_{TGA}$ ) together with its  
 283 experimental uncertainty, and the estimated value obtained from the model proposed ( $MR_{mod}$ )  
 284 can be observed in Figure 7 a). The experimental uncertainty of the measurement of the  
 285 moisture ratio in the TGA (shown in grey in Figure 7 a)) is reduced due to the high precision in  
 286 the mass measurement. As can be seen in Figure 7 a), the model follows the trend of the  
 287 evolution of the moisture ratio of the apples for a drying process with a variable temperature.  
 288 In fact, the deviation between the model estimation of the drying time ( $t_d$ ) and the  
 289 experimental values is lower than 2.5 min for moisture ratios between 1 and 0.1, as shown in  
 290 Figure 7 b). This maximum deviation of 2.5 min corresponds to a maximum relative error of the  
 291 time estimated by the model of 1.5%. Nevertheless, the estimation of the moisture ratio  
 292 performed by the model is inside the low range of uncertainty of the measurement of the TGA.  
 293 Therefore, the model was proved to predict accurately the evolution of the moisture ratio  
 294 during a variable temperature thin-layer drying process of Granny Smith apples.”



295  
 296 Figure 7: a) Measured and estimated evolution of the moisture ratio with time for the variable  
 297 temperature drying process in the TGA, b) deviation between the estimated and the measured  
 298 drying time.

299 **4.2. Application of the drying model in an indirect solar dryer**

300 Once validated using TGA measurements, the model was applied to the drying of Granny Smith  
 301 apples in a solar indirect dryer. In this case, a total mass of around 80 g of slices of apples (2.4  
 302 mm in thickness) were dried on the reference tray in the drying chamber. The variation of the  
 303 sample mass with time was measured with the balance each 5 s. Therefore, the evolution of the  
 304 the moisture ratio with time during the drying process in the indirect solar dryer can be  
 305 calculated, and a procedure similar to that employed previously for the TGA measurements  
 306 can be followed. First, several constant temperature drying tests were performed in the  
 307 indirect solar dryer, using temperatures between 25 °C and 40 °C in intervals of 5 °C. In this  
 308 case, for each value of the temperature, the corresponding value of the relative humidity of air  
 309 was employed, following the weather data for the reference climate and the drying conditions  
 310 explained in Section 2. The evolution with time of the moisture ratio obtained in the solar  
 311 dryer for each temperature is plotted in Figure 8. An increase in the constant temperature of  
 312 the drying process decreases significantly the drying time, similar to what was shown for the  
 313 TGA experiments.



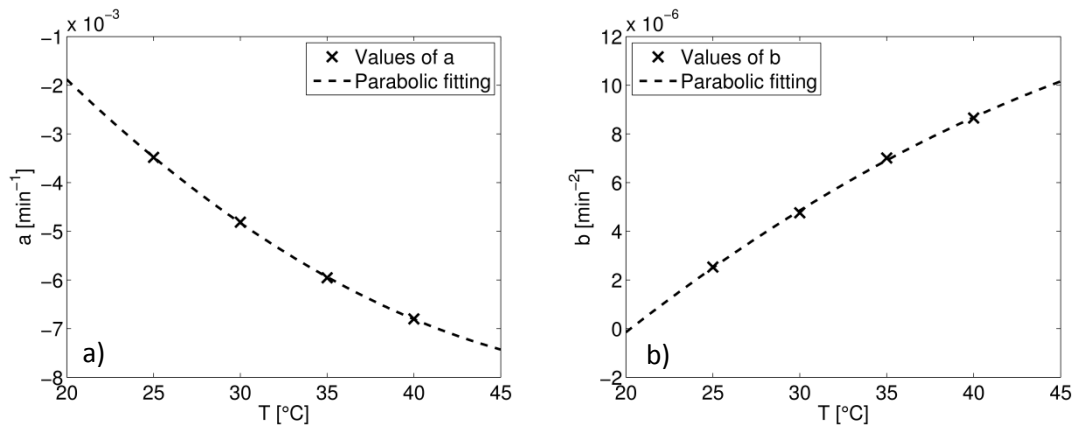
314 Figure 8: Evolution of the moisture ratio with time during the thin-layer drying of Granny Smith  
 315 apples in an indirect solar dryer.  
 316

317 The moisture ratio curves obtained for each constant temperature in the indirect solar dryer  
 318 were fitted to a curve as that proposed by Wang and Singh [29], shown in Eq. 5, determining  
 319 the fitting parameters  $a$  and  $b$ . The values of the fitting parameters obtained for each  
 320 temperature are presented in Figure 9, together with their parabolic fitting. The equations of  
 321 the parabolic fitting of the parameters  $a$  and  $b$  of the Wang-Singh equation for the thin-layer  
 322 drying of Granny Smith apples in the solar indirect dryer, considering the drying conditions  
 323 explained in Section 2, are:

$$324 \quad a_{SD} = 4.86 \cdot 10^{-6} T^2 - 5.38 \cdot 10^{-4} T + 6.93 \cdot 10^{-3} \quad (8)$$

$$325 \quad b_{SD} = -5.87 \cdot 10^{-9} T^2 + 7.94 \cdot 10^{-7} T - 1.37 \cdot 10^{-5} \quad (9)$$

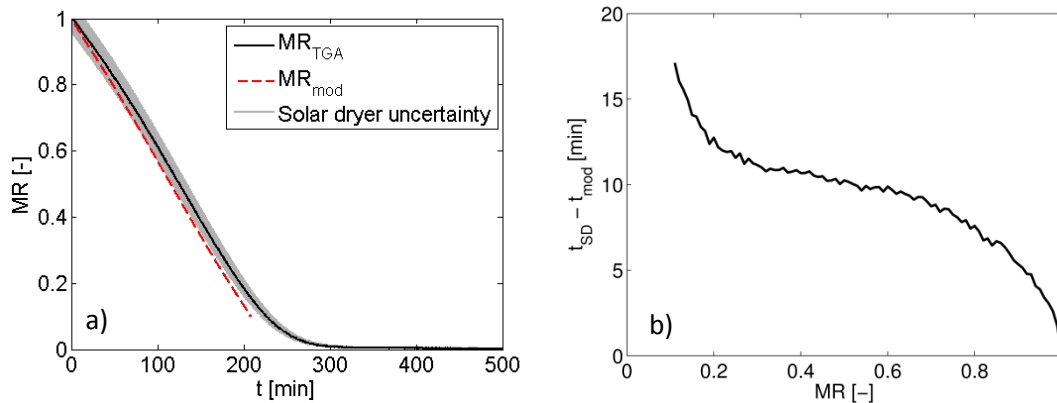
326 where  $a_{SD}$  is obtained in  $\text{min}^{-1}$  and  $b_{SD}$  in  $\text{min}^{-2}$  for a temperature  $T$  in °C.



327  
 328 Figure 9: Values of the parameters of the equation proposed by Wang and Singh [29] for the  
 329 indirect solar dryer measurements.

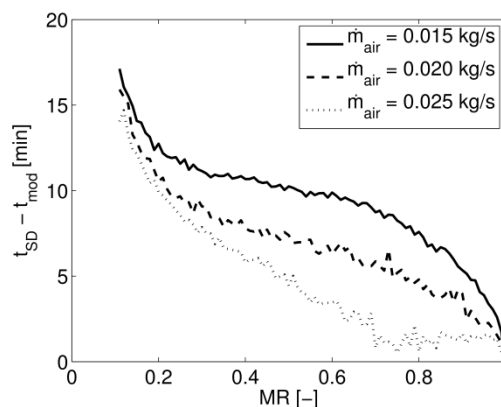
330 The model proposed for the thin-layer drying of Granny Smith apples at variable temperature  
 331 was applied to the drying process in the solar indirect dryer. To that end, the values of the  
 332 parameters  $a_{SD}$  and  $b_{SD}$  of the Wang-Singh equation for the solar dryer were obtained from Eq.  
 333 8 and Eq. 9 for each drying chamber temperature. The drying chamber temperature was that  
 334 showed in Figure 3. Then, using the variable temperature and the parabolic fittings of the  
 335 parameters  $a_{SD}$  and  $b_{SD}$  for the solar dryer, the proposed model can be employed to estimate  
 336 the evolution of the moisture ratio with time during the thin-layer drying of Granny Smith  
 337 apples. The values measured in the indirect solar dryer for the moisture ratio are shown in  
 338 Figure 10 a), together with their uncertainty and the estimation of the model. The  
 339 experimental curve showed in Figure 10 a) is the average of 4 different tests. Nevertheless, the  
 340 tests present high repeatability, being the maximum deviation in the whole  $MR$  curve less than  
 341 0.01. In each test, 9 slices of apple were dried in the reference mesh detailed in section 2.2. In  
 342 this case, the uncertainty associated to the measurement of the moisture ratio is higher than  
 343 in the TGA, as a consequence of the lower weighing precision of the indirect solar dryer.

344 The model seems to overestimate the drying capacity of the solar indirect dryer, predicting  
 345 lower drying times than those measured, falling even out of the uncertainty range of the  
 346 experimental measurement for low values of the moisture ratio. The maximum deviation  
 347 between the predicted and the measured drying time for the indirect solar dryer was lower  
 348 than 20 min, as shown in Figure 10 b), corresponding to a maximum relative error around 10%.  
 349 The higher error obtained for the estimations of the model for the drying process occurring in  
 350 the indirect solar dryer might be attributed to the effect of the thermal inertia of the sample.  
 351 For the experiments in the indirect solar dryer, the mass of the sample is much larger than the  
 352 mass used in the TGA tests (approximately 80 g in the indirect solar dryer and just around 150  
 353 mg in the TGA), thus the temperature of the sample might differ from that measured in the air  
 354 of the drying chamber. The lower temperature of the sample in the indirect solar dryer tests  
 355 due to thermal inertia would delay the drying process, producing the differences observed in  
 356 Figure 10.



357  
 358 Figure 10: a) Measured and estimated evolution of the moisture ratio with time for the  
 359 variable temperature drying process in the indirect solar dryer, b) deviation between the  
 360 estimated and the measured drying time.

361 The effect of the thermal inertia of the sample on the delay of the drying process in the  
 362 indirect solar dryer was analyzed performing drying tests using the atmospheric conditions  
 363 described in Section 2 for various air mass flow rates. The nominal air mass flow rate of 0.015  
 364 kg/s was increased to 0.020 and 0.025 kg/s and drying tests were carried out. The process to  
 365 obtain the estimations of the model proposed for the moisture ratio evolution was repeated  
 366 for these new values of the air mass flow rate, and the deviations in time between the  
 367 experimental measurements and the model predictions were quantified. The results are  
 368 shown in Figure 11, where the time deviations for the three different air mass flow rates  
 369 employed are plotted. The deviations are proved to decrease for higher air mass flow rates, as  
 370 a consequence of the higher convection coefficient obtained using a higher air velocity, which  
 371 reduces the effect of thermal inertia of the sample. In fact, the estimation of the model for the  
 372 moisture ratio using an air mass flow rate of 0.025 kg/s falls inside the uncertainty associated  
 373 to the experimental measurement.



374  
 375 Figure 11: Deviation between the estimated and the measured drying time for different values  
 376 of the air mass flow rate.

### 377 5. Conclusions

378 The kinetics of the thin-layer drying process of Granny Smith apples was experimentally  
 379 analysed by means of thermogravimetric measurements. Drying tests were conducted at  
 380 different constant drying temperatures in a TGA, obtaining the drying curves of Granny Smith

381 apples as a function of temperature. The Wang-Singh equation was employed to fit the  
382 experimental drying curves obtained in the TGA for constant temperatures. A novel model was  
383 proposed, based on the Wang-Singh equation, to predict the evolution of the moisture ratio  
384 during the thin-layer drying process of Granny Smith apples under variable temperature  
385 profiles. The model was validated using experimental results of the drying of apples in the TGA  
386 for a variable drying temperature. The prediction of the model proposed for the evolution of  
387 the moisture ratio with variable temperature was in excellent agreement with the  
388 experimental measurements obtained in the TGA, obtaining a maximum deviation from the  
389 experiments of 1.5%, a deviation which is inside the uncertainty associated with the  
390 measurements.

391 The model was also applied to the drying process of thin slices of Granny Smith apples in an  
392 indirect solar dryer. The procedure was replicated, obtaining the parameters of the Wang-  
393 Singh equation for the drying conditions presented in the solar drying process. The comparison  
394 of the model estimations with experimental measurements carried out in a lab-scale indirect  
395 solar dryer shows a proper agreement, obtaining deviations under 10%. Nevertheless, the  
396 experimental values of the moisture ratio were delayed compared to the model predictions, a  
397 result that can be attributed to the effect of the thermal inertia of the sample in the indirect  
398 solar dryer. This effect was proved increasing the air mass flow rate, obtaining in this case a  
399 prediction of the moisture rate from the model that falls inside the uncertainty range  
400 associated with the experimental measurement.

#### 401 **Acknowledgements**

402 The thermogravimetric analyses were conducted in the BIOLAB experimental facility  
403 (madrimsd.org, lab # 202), a laboratory financed under the infrastructures and lab network of  
404 the Madrid (Spain) Regional Government.

#### 405 **Nomenclature**

406  $A_c$ – Solar collector area [ $\text{m}^2$ ].

407  $a$ – Free parameter in the Wang-Singh equation [ $\text{s}^{-1}$ ].

408  $b$ – Free parameter in the Wang-Singh equation [ $\text{s}^{-2}$ ].

409  $c_p$  – Specific heat of the air [ $\text{J kg}^{-1} \text{K}^{-1}$ ]

410  $dt$  – Time interval [s].

411  $I$  – Solar irradiance on the horizontal plane [ $\text{W m}^{-2}$ ].

412  $I_T$  – Solar irradiance on the collector angle [ $\text{W m}^{-2}$ ].

413  $\dot{m}_{air}$  – Air mass flow rate [ $\text{kg s}^{-1}$ ].

414  $M$  – Moisture content as a function of time (wet basis) [ $\text{kg kg}^{-1}$ ].

415  $M_e$  – Equilibrium moisture content (wet basis) [ $\text{kg kg}^{-1}$ ].



416  $M_0$  – Initial moisture content (wet basis) [ $\text{kg kg}^{-1}$ ].

417  $MR$  – Moisture ratio [-].

418  $R_b$  – Ratio of beam irradiance on tilted surface to that on the horizontal plane [-].

419  $S$  – Solar irradiance absorbed by the absorber plate [ $\text{W m}^{-2}$ ].

420  $T$  – Temperature [ $^{\circ}\text{C}$ ].

421  $t$  – Time [s].

422  $t_d$  – Drying time [s].

423 **Greek letters**

424  $\beta$  – Angle of inclination of the solar collector [ $^{\circ}$ ].

425  $\Delta MR$  – Moisture ratio reduction [-].

426  $\rho_g$  – Ground reflectance [-]

427  $(\tau\alpha)$  – Effective transmittance-absorptance product [-].

428  $\phi$  – Relative humidity [-].

429 **Subscripts**

430  $0$  – Inlet of the collector

431  $1$  – Outlet of the collector, inlet of the drying chamber

432  $b$  – Beam component

433  $d$  – Diffuse component

434  $g$  – Ground reflection

435  $mod$  – Model

436  $SD$  – Solar dryer

437  $TGA$  – Thermogravimetric analyzer

438 **References**

439 [1] Kumar, M., Sansaniwal, M.K, Khatak, P., Progress in solar dryers for drying various  
440 commodities. Renewable and Sustainable Energy Reviews, 2016, 55, 346-360.

441 [2] Fudholi, A., Sopian, K., Ruslan, M.H., Alghoul, M.A., Sulaiman, M.Y. Review of solar dryers  
442 for agricultural and marine products. Renewable and Sustainable Energy Reviews, 2010, 14, 1-  
443 30.

- 444 [3] Gulcimen F., Karakaya H., Durmus A. Drying of sweet basil with solar air collectors,  
445 Renewable Energy, 2016, 93, 77-86.
- 446 [4] Velic, D., Planinic, M., Tomas, S., Bilic, M. Influence of airflow velocity on kinetics of  
447 convection apple drying. Journal of Food Engineering, 2004, 64, 97-102.
- 448 [5] Vega-Gálvez, A., Ah-Hen, K., Chacana, M., Vergara, J., Martínez-Monzó, J., García-Segovia,  
449 P., Lemus-Mondaca, R., Di Scala, K. Effect of temperature and air velocity on drying kinetics,  
450 antioxidant capacity, total phenolic content, colour, texture and microstructure of apple. Food  
451 Chemistry, 2012, 132, 51-59.
- 452 [6] Romano, G., Kocsis, L., Farkas, I. Analysis of energy and environmental parameters during  
453 solar cabinet drying of apple and carrot. Drying Technology, 2009, 27, 574-579.
- 454 [7] Lamnatoua, C., Papanicolaou, E., Belessiotis, V., Kyriakis, N. Experimental investigation and  
455 thermodynamic performance analysis of a solar dryer using an evacuated-tube air collector.  
456 Applied Energy, 2012, 94, 232-243.
- 457 [8] Elicin, A.K., Sacilik K. An experimental study for solar tunnel drying of apple. Tarim Bilimleri,  
458 2005, 11(2), 207-211.
- 459 [9] Blanco-Cano, L., Soria-Verdugo, A., Garcia-Gutierrez, L.M., Ruiz-Rivas, U. Evaluation of the  
460 maximum evaporation rate in small-scale indirect solar dryers. ASME Journal of Solar Energy  
461 Engineering, 2016, 138, 0245021-0245024.
- 462 [10] Akpınar, E.K., Yasar, B. Modelling of the drying of eggplants in thin-layers. International  
463 Journal of Food Science and Technology, 2005, 40, 273–281.
- 464 [11] Zhu, A., Shen, X. The model and mass transfer characteristics of convection drying of  
465 peach slices. International Journal of Heat and Mass Transfer, 2014, 72, 345-351.
- 466 [12] Doymaz, I. An experimental study on drying of green apples. Drying Technology, 2009, 27,  
467 478-485.
- 468 [13] Celma, A.R., Rojas, S., López, F., Montero, I., Miranda, T. Thin-layer drying behaviour of  
469 sludge of olive oil extraction. Journal of Food Engineering, 2007, 80 (4), 1261-271.
- 470 [14] Basunia, M.A., Abe, T. Thin-layer solar drying characteristics of rough rice under natural  
471 convection. Journal of Food Engineering, 2001, 47, 295-301.
- 472 [15] Aktaş M., Ceylan I., Yılmaz S. Determination of drying characteristics of apples in a heat  
473 pump and solar dryer. Desalination, 2009, 239 (1-3), 266-275.
- 474 [16] Janjai, S., Lamlert, N., Intawee, P., Mahayothee, B., Bala, B.K., NagleM., Muller, J.  
475 Experimental and simulated performance of a PV-ventilated solar greenhouse dryer for drying  
476 of peeled longan and banana, Solar Energy, 2009, 83, 1550-1565.
- 477 [17] Karim, M.A., Hawlader, M.N.A. Drying characteristics of banana: theoretical modelling and  
478 experimental validation. Journal of Food Engineering, 2005, 70, 35-45.

- 479 [18] Sacilik, K., Elicin, A.K. The thin layer drying characteristics of organic apple slices. *Journal of*  
480 *Food Engineering*, 2006, 73, 281-289.
- 481 [19] Menges, H.O., Ertekin, C. Mathematical modelling of thin layer drying of Golden apples.  
482 *Journal of Food Engineering*, 2006, 77, 119-125.
- 483 [20] Zlatanovic, I., Komatina, M., Antonijevic, D. Low-temperature convective drying of apple  
484 cubes. *Applied Thermal Engineering*, 2013, 53, 114-123.
- 485 [21] Sturm B., Nunez Vega A.M., Hofacker, W. C. Influence of process control strategies on  
486 drying kinetics, colour and shrinkage of air dried apples, *Applied Thermal Engineering*, 2014, 62  
487 (2), 455-460.
- 488 [22] Velic, D., Bilic, M., Tomas, S., Planinic, M., Bucic-Kojic, A., Aladic, K. Study of the drying  
489 kinetics of "Granny Smith" apple in tray drier. *Agriculturae Conspectus Scientificus*, 2007, 72  
490 (4), 323-328.
- 491 [23] González-Fésler, M., Salvatori, D., Gómez, P., Alzamora, S.M. Convective air drying of  
492 apples as affected by blanching and calcium impregnation. *Journal of Food Engineering*, 2008,  
493 87, 323-332.
- 494 [24] Iglesias, I., Carbó, J., Bonany, J., Montserrat, R. Varietal innovation in apples. *Revista de*  
495 *Fruticultura*, 2009, 1 (10), 13-25.
- 496 [25] Energy Plus. Weather Data. <https://energyplus.net/weather> Last access: Feb 2016.
- 497 [26] Duffie, J.A., Beckman, W.A. *Solar Engineering of Thermal Processes*. John Wiley and Sons.  
498 Hoboken, New Jersey, 2006. Third Edition.
- 499 [27] Ekechukwu, O.V., Norton, B. Review of solar-energy drying systems III: low temperature  
500 air-heating solar collectors for crop drying applications. *Energy Conversion and Management*,  
501 1999, 4, 657-667.
- 502 [28] Panchariya P.C., Popovic, D., Sharma, A.L. Thin-layer modelling of black tea drying  
503 process. *Journal of Food Engineering*, 2002, 52, 349-357.
- 504 [29] Wang, C.Y., and Singh, R.P. A single layer drying equation for rough rice. ASAE, 1978, paper  
505 No: 78-3001, ASAE, St. Joseph, MI.
- 506 [30] Lewis, W.K. The Rate of Drying of Solid Materials. *The Journal of Industrial and Engineering*  
507 *Chemistry*, 1921, 13(5), 427-432.
- 508 [31] Page, G. Factors influencing the maximum rates of air drying shelled corn in layers. M. S.  
509 thesis, 1949, Purdue University.
- 510 [32] Henderson, S.M. and Pabis, S. Grain drying theory. I. Temperature effect on drying  
511 coefficient. *Journal of Agricultural Engineering Research*, 1961, 6(3), 169-174.
- 512 [33] Madamba, P.S., Driscoll, R.H., Buckle, K.A. The thin layer drying characteristics of garlic  
513 slices. *Journal of Food Engineering*, 1996, 29, 75-97.

- 514 [34] Ertekin, C., Yaldiz, O. Drying of eggplant and selection of a suitable thin layer drying model.  
515 Journal of Food Engineering, 2004, 63, 349-359.
- 516 [35] Togrul, I.T., Pehlivan, D. Mathematical modeling of solar drying of apricots in thin layers.  
517 Journal of Food Engineering, 2002, 55, 209-216.
- 518 [36] Verma, L.R., Bucklin, R.A., Endan, J.B., Wratten, F.T. Effects of drying air parameters on  
519 rice drying models. Transactions of the ASAE, 1985, 28, 296-301.
- 520 [37] Karathanos, V.T. Determination of water content of dried fruits by drying kinetics. Journal  
521 of Food Engineering, 1999, 39, 337-344.
- 522 [38] Midilli, A., Kucuk, H, Yapar, Z. A new model for single layer drying. Drying Technology,  
523 2002, 20(7), 1503-1513.